PUBLICATIONS OF THE ASTRONOMICAL SOCIETY OF THE PACIFIC, 111:571–586, 1999 May

Spectroscopic Observations of Some S-Type Symbiotic Stars

A. GUTIÉRREZ-MORENO, H. MORENO,[1] AND E. COSTA[1]

Departamento de Astronomía, Universidad de Chile, Casilla 36-D, Santiago, Chile; agutierr@das.uchile.cl, hmoreno@das.uchile.cl, ecosta@das.uchile.cl

Received 1998 November 4; accepted 1999 January 13

ABSTRACT. Observations of a group of S-type symbiotic stars are presented: Hen 828, Hen 905, Hen 1103, Hen 1213, KX TrA (Cn 1-2), AE Ara (PC 18), AS 255, AS 270, AS 289, Y CrA, AS 304, AS 316, AS 327, and CD $-43°14304$. The observations were made in three different epochs of observation: 1987, 1991, and 1995, except for Y CrA, which was observed in 1990. Several parameters are obtained for each object: spectral types of the late components; distances derived from these spectral types; interstellar reddening as determined from the Balmer decrement, considering optical depth effects; electron temperatures and densities; helium abundances, also determined considering optical depth effects; and characteristics of the hot components.

It has been found that Hen 828 and Hen 1103 were possibly having an outburst in 1991; the same could be true for AS 270 in 1995 and CD $-43°14304$ in 1991. Another interesting object is Hen 905, which is surrounded by a nebulosity that could be a ring, reaching a distance of about 2′, with emission mainly in Hα and O VI λ6825.

1. INTRODUCTION

Symbiotic stars are interacting binary systems with three components: an evolved cool giant clearly seen in the red part of the optical spectrum, a hot radiation source, and an ionized nebula that is conspicuous because of its emission lines. The hot component can be a wind-accreting white dwarf, a hot subdwarf, or a disk-accreting main-sequence star; its physical characteristics are similar to those of the central stars of planetary nebulae, with $T^* \approx 10^4$–10^5 K and $\log L^* = 10^3$–$10^4\ L_\odot$.

According to the evidence of dust deduced from the near-infrared colors, symbiotic stars have been divided (Allen 1982a, 1982b) in two major types: S types, which are characterized by their IR continua, showing only the presence of a cool star; and D and D′ types, which are characterized by infrared radiation dominated by dust with temperatures of the order of 800–1000 K for D type, or half as great for the D′ type (Allen 1982a, 1982b). S-type systems contain high-density nebulae ($N_e \geq 10^7$ cm^{-3}) ionized by a hot source with $T^* > 70{,}000$ K. D and D′ types have lower density nebulae ($N_e \leq 10^7$ cm^{-3}) and hot sources of lower temperature ($T^* \approx 60{,}000$ K).

In a previous paper Gutiérrez-Moreno, Moreno, & Cortés (1995) presented a diagnostic diagram adequate for separating planetary nebulae from symbiotic stars, based only on the behavior of the [O III] lines in the optical region. Besides, the diagram separates very well the D- and S-type symbiotic objects, showing that D- and D′-type systems have densities of the order of 10^6–10^7 cm^{-1}, whereas S-type systems have densities larger than 10^7 cm^{-1}, coming close to the high-density limit. Several symbiotic stars were observed with the aim of obtaining this diagram. We have already presented an analysis of the observations of a group of symbiotic stars of D and D′ type (Gutiérrez-Moreno & Moreno 1996); in this paper we present a similar analysis of the observations of some S-type symbiotic stars.

2. OBSERVATIONS AND REDUCTIONS

Details of the objects observed are given in Table 1, which lists, by column, (1) and (2) the name or names of the objects observed; (3) and (4) their positions referred to the equinox 2000.0; (5)–(8) the magnitude K and the colors $J-H$, $H-K$, and $K-L$, taken from Munari et al. (1992) except when indicated; and (9) the spectral types of the late components as listed by Whitelock & Munari (1992).

The observations were made in five different runs; the details concerning the instrumentation used are listed in Table 2, which is self-explanatory. Table 3 indicates the observing runs corresponding to each object.

For all the observations the slit was oriented in the east-west direction. All the objects were observed through a

[1] Visiting Astronomer, Cerro Tololo Inter-American Observatory, National Optical Astronomy Observatories, operated by the Association of Universities for Research in Astronomy (AURA), Inc., under cooperative agreement with the National Science Foundation.

TABLE 1

OBSERVED OBJECTS

Name (1)	Other (2)	R.A. (2000.0) (3)	Decl. (2000.0) (4)	K (5)	$J-H$ (6)	$H-K$ (7)	$K-L$ (8)	Spectral Type (9)
Hen 828		12 50 58.0	−57 50 46	7.17	1.10	0.38	...	M6
Hen 905		13 30 37.2	−57 58 17	8.39	1.12	0.35	...	K4:
Hen 1103		15 48 28.4	−44 19 00	8.40	1.00	0.30	...	M0
Hen 1213[a]		16 35 15.2	−51 42 24	6.72	1.08	0.29	...	K4
KX TrA	Cn 1-2, Hen 1242	16 44 35.5	−62 37 13	5.99	1.03	0.35	0.37	M6
AE Ara	PC 18	17 41 04.9	−47 03 20	6.48	1.01	0.30	0.23:	M2
AS 255	Hen 1525	17 57 08.8	−35 15 34	8.25	0.88	0.23	...	K3
AS 270	Hen 1581	18 05 33.7	−20 20 34	5.65	1.33	0.42	0.28	M1
AS 289	Hen 1627	18 12 22.2	−11 40 07	5.04	1.28	0.46	0.42	M3.9
Y CrA[a]	HD 166813	18 14 22.9	−42 50 30	6.54	0.98	0.35	...	M5
AS 304	Hen 1691	18 25 26.7	−28 35 57	7.40	0.88	0.31	...	M4
AS 316[a]	Hen 2-417	18 42 32.8	−21 17 47	7.76	...	0.31	...	M
AS 327	Hen 1730	18 53 16.7	−24 22 57	7.62	1.07	0.27	...	M4
CD −43°14304	Hen 1924	21 00 06.3	−42 38 50	7.60	0.90	0.18	...	K5.5

NOTE.—Units of right ascension are hours, minutes, and seconds, and units of declination are degrees, arcminutes, and arcseconds.

[a] Infrared values taken from Allen 1982a, 1982b.

narrow slit (3″–5″), to obtain the best spectral resolution, and through a wide slit (≈ 10″), to obtain accurate spectrophotometry. The standard stars were taken from Stone & Baldwin (1983) for the Two Degree Field (2dF) observations, from Taylor (1984) for the 1991 CCD observations, and from Stone & Baldwin (1983) as improved by Hamuy et al. (1992) for the 1995 CCD observations. The standard stars were always observed with the wide slit.

The data reductions were performed at the Cerro Tololo Inter-American Observatory (CTIO) La Serena Computing Center. All the observations were reduced to linear wavelength and flux scales using the program IRAF (Image Reduction Analysis Facilities).[2] The spectra thus obtained were then measured using the task SPLOT in IRAF, on Sun workstations available at the Centro de Procesamiento Digital de Imágenes (CPDI) of the Departamento de Astronomía de la Universidad de Chile; the blends were resolved using the DEBLEND option in the task SPLOT. When the spectra were obtained through both a narrow and a wide slit with the same equipment, the narrow spectra were reduced to the wide spectra without losing resolution; in this way, differences in the continuum or line intensities obtained in different epochs of observation cannot be attributed to differences in the slit widths.

The spectra of all the objects observed are presented in Figures 1–14.

The measured fluxes relative to Hβ are listed in Table 4; the last line of the table gives the logarithm of the observed flux in Hβ. No individual mean internal errors are given for the different lines observed, but an analysis of the fluxes measured for the same object from different spectra obtained during the same night shows that they may be

[2] IRAF is distributed by National Optical Astronomical Observatories, which is operated by the Association of Universities for Research in Astronomy, Inc., under contract to the National Science Foundation.

TABLE 2

INSTRUMENTATION IN THE DIFFERENT OBSERVING RUNS

Run	Date	Telescope	Detector	Wavelength Range (Å)	FWHM (Å)	Filter
1	1987 Jul	1.0 m	2dF	3200–7100	5	WG 360
2a	1990 Jun	1.5 m	GEC CCD	3100–7600	17	...
2b	1990 Jun	1.5 m	GEC CCD	6100–10400	16	RG 610
3a	1991 Jun	1.0 m	2dF	3200–7100	5	...
3b	1991 Jun	1.0 m	2dF	4300–7800	5	GG 455
4a	1991 Jul	1.5 m	GEC CCD	3200–7700	17	...
4b	1991 Jul	1.5 m	GEC CCD	6100–10400	16	RG 610
5a	1995 Apr	1.5 m	GEC CCD	4000–5400	5	...
5b	1995 Apr	1.5 m	GEC CCD	4600–7100	9	GG 455

TABLE 3

OBSERVING RUNS FOR THE DIFFERENT OBJECTS

	Run								
	1987	1990		1991 Jun		1991 Jul		1995	
Object	1	2a	2b	3a	3b	4a	4b	5a	5b
Hen 828	+					+	+		
Hen 905	+								
Hen 1103	+					+	+		
Hen 1213	+			+	+			+	+
KX TrA	+								
AE Ara						+	+		
AS 255	+					+	+		
AS 270	+					+	+	+	+
AS 289	+			+	+				
Y CrA		+	+						
AS 304	+								
AS 316	+					+			
AS 327	+					+			
CD −43°14304	+			+	+	+	+		

estimated as $\leq 10\%$ for well-separated lines with $\log F(\lambda) > -12$, increasing up to about 50% for blended lines or for lines with $\log F(\lambda) \leq -14$. The error determined for $\log F(\mathrm{H}\beta)$ is in all cases of the order of 0.1 dex. The true errors may be quite larger, considering possible errors in the calibrations and in the atmospheric extinction curves adopted and the difficulties in the tracing of the continuum due to the noise and to the presence of absorption bands.

For the determination of the physical parameters deduced from these fluxes, the lines of the Balmer series have been corrected for the contamination produced by the Pickering series of He II. Besides, Hα has been corrected for the contamination produced by He II Pf 14.

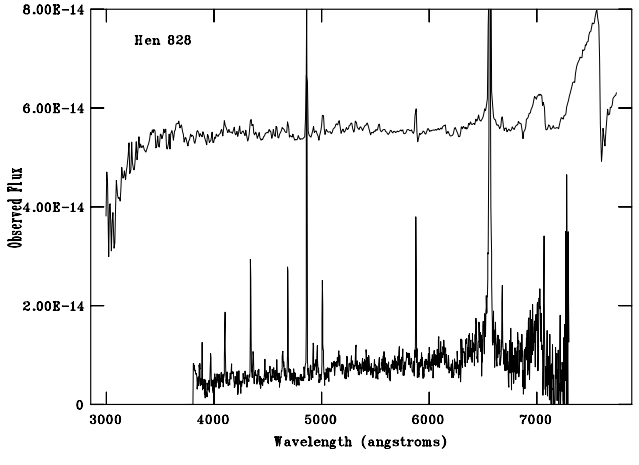

FIG. 1.—Spectra of Hen 828. Here and in all the figures that follow the spectra obtained at the earliest date are at the bottom, and those obtained at the latest date are at the top. The ordinates and the separation steps are in ergs $\mathrm{cm}^{-2}\ \mathrm{s}^{-1}$; the spectra corresponding to 1991 are combined spectra, including the red and blue observations. Here the separation step is 4×10^{-14}.

3. THE LATE COMPONENTS

The spectral types of the late components were obtained—assuming that they are all giants—by the $[\mathrm{TiO}]_1$, $[\mathrm{TiO}]_2$, and [VO] indices given by Kenyon & Fernández-Castro (1987) and by the [TiO] index given by Kenyon (1986); the indexes presented by Terndrup, Frogel, & Whitford (1990) were also used. The determinations were made separately for each period of observations. When the spectral type seemed to be dependent of the wavelength of the features used, the latest spectral type obtained for each object was adopted, because of the possibility that the

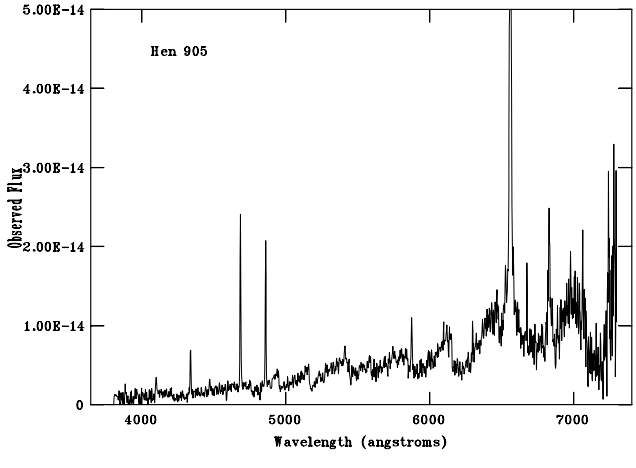

FIG. 2.—Spectrum of Hen 905 obtained in 1987

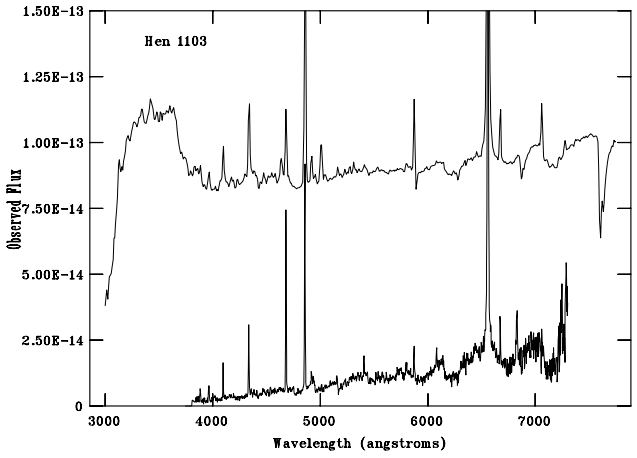

FIG. 3.—Spectra of Hen 1103. Notice the intensity of the Balmer continuum in emission in 1991. The separation step is 4×10^{-14}.

absorption bands are being veiled in some cases by the nebular component. The final spectral type adopted was confirmed by visual comparison with the digital spectra published by Turnshek et al. (1985). In general, the differences between the types obtained for a given object in different periods are within what may be considered the errors of the observations, and the average of the different classifications has been adopted.

The knowledge of the spectral types allows an estimate of the distance of the different objects. The absolute K magnitudes used for the M giants were obtained from the calibration of the M giants located in the Galactic bulge made by Frogel & Whitford (1987), using a distance to the center of the Galaxy equal to 8.3 kpc. The observed K magnitudes were taken from Table 1, and the corresponding A_K absorptions were taken from Table 6 of the next section.

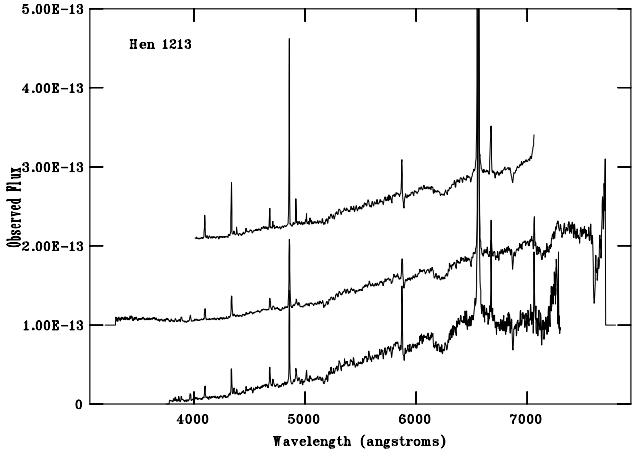

FIG. 4.—Spectra of Hen 1213. The separation step is 1×10^{-13}. In 1991 there is a hint that the Balmer continuum is in emission. All the observations are made with the same slit width, which allows a direct comparison of the lines intensities. In the 1995 spectrum, the greater strength of the emission lines of the Balmer series, is noticeable.

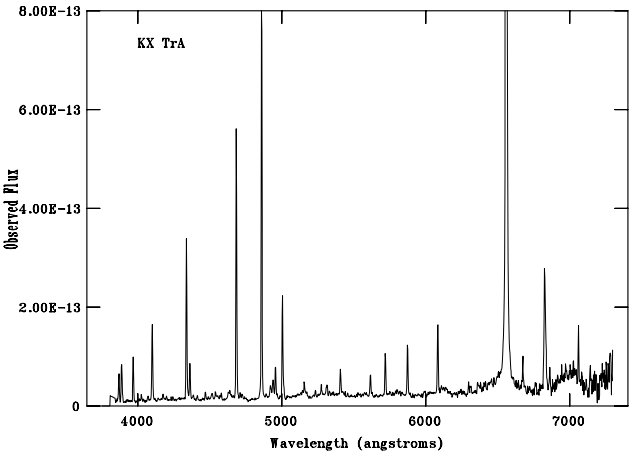

FIG. 5.—High-excitation spectrum of KX TrA (Cn 1-2) obtained in 1987.

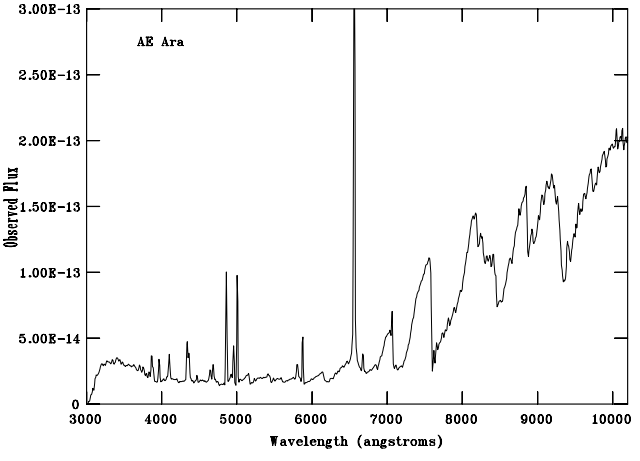

FIG. 6.—Combined spectrum of AE Ara obtained in 1991. The Balmer continuum is in emission.

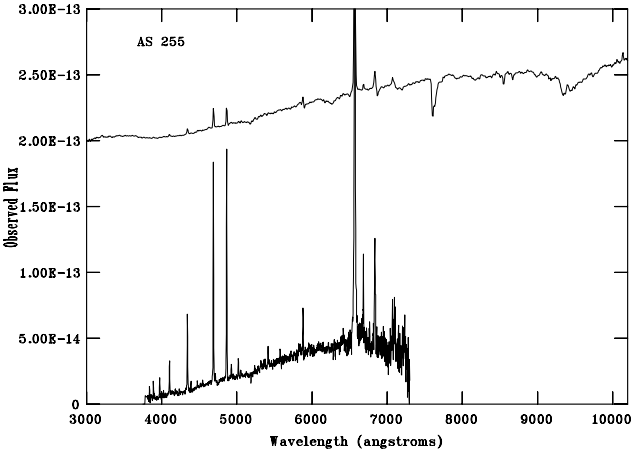

FIG. 7.—Spectra of AS 255. The separation step is 2×10^{-13}. The emission lines are more intense in 1987 than in 1991. In 1991 the Balmer continuum can be see faintly in emission.

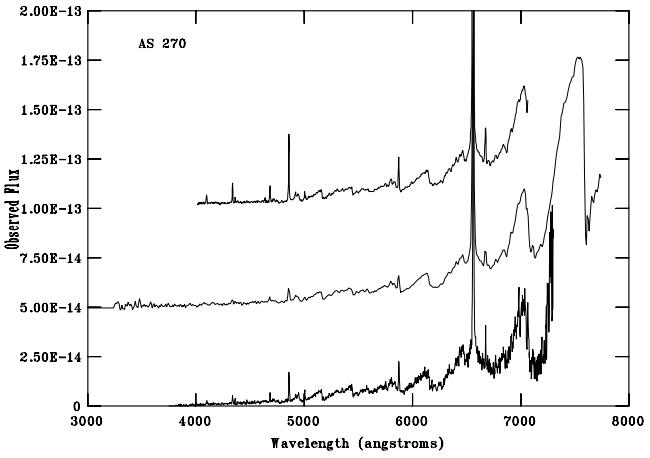

FIG. 8.—Spectra of AS 270. The separation step is 5×10^{-14}. The difference in the intensity of the emission lines, mainly of the Balmer lines, is noticeable.

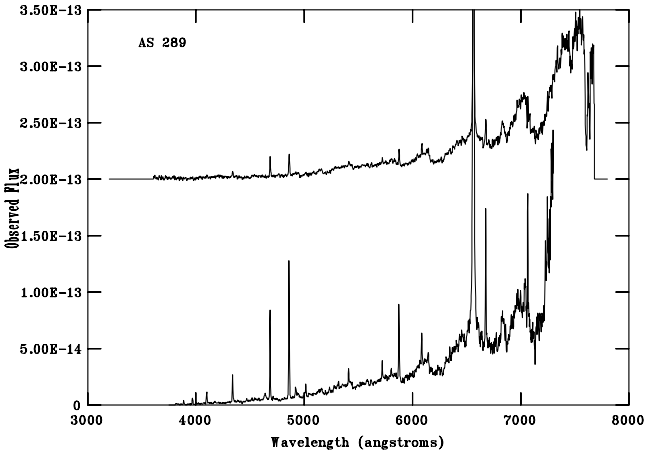

FIG. 9.—Spectra of AS 289. The separation step is 2×10^{-13}. As in Fig. 4, both spectra were obtained with the same slit width. The emission lines are much more intense in 1987 than in 1991. Notice the strength and width of λ6825.

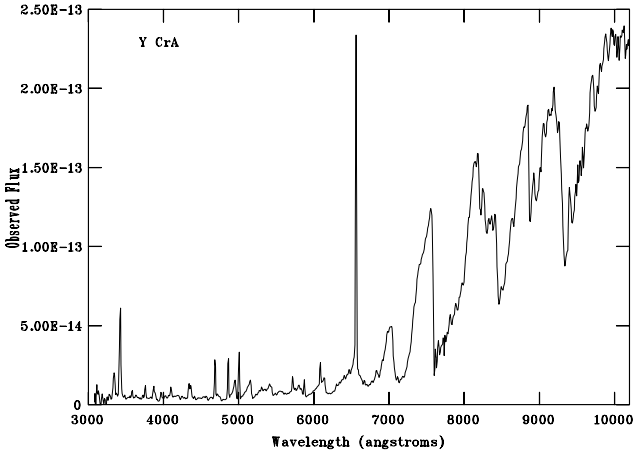

FIG. 10.—Combined spectrum of Y CrA, obtained in 1990

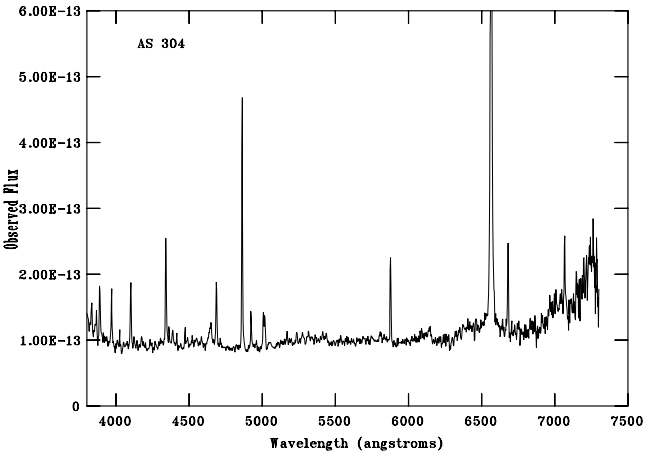

FIG. 11.—Spectrum of AS 304 obtained in 1987

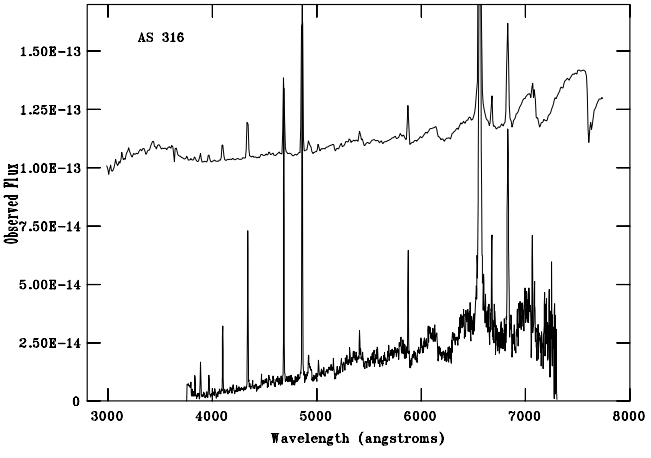

FIG. 12.—Spectra of AS 316. The separation step is 2×10^{-13}.

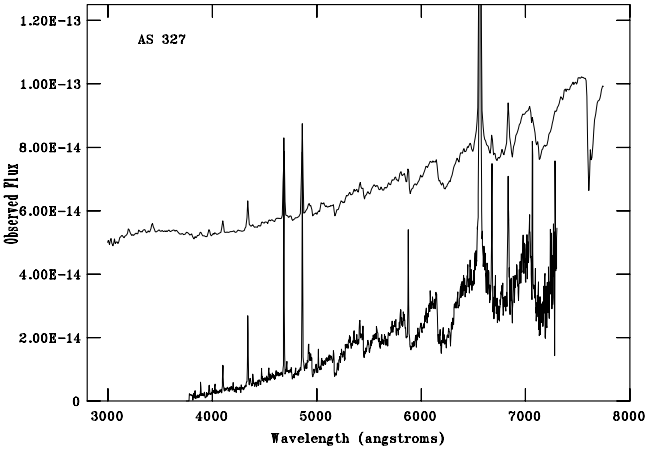

FIG. 13.—Spectra of AS 327. The separation step is 1×10^{-13}. In spite of the difference in the slit widths for the two spectra presented here, the difference in the strength of the He lines, mainly of λ5876, is noticeable.

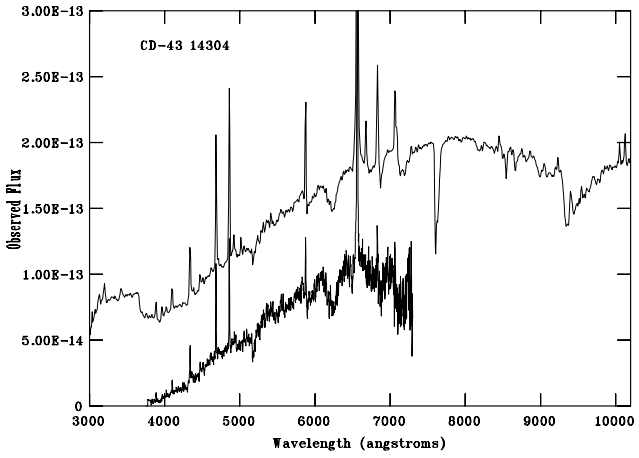

FIG. 14.—Spectra of CD −43°14304. Notice the Balmer discontinuity in emission.

The results are listed in Table 5, which gives, by column, (1) the name of the object, (2) the spectral type with its mean error, (3) the spectral types listed by other authors, (4) the distances obtained in this paper, and (5) the distances listed by other authors.

The internal errors of the distances corresponding to our internal errors in the spectral types and in the reddenings are small, running from 0.1 to 0.4 kpc. But the main errors originate in the adequacy of the calibration used and in the accuracy of the calibration, which we cannot evaluate.

4. THE NEBULAR COMPONENT

4.1. Reddening, Optical Depth, and Related Parameters

The reddening constants Cβ and the optical depths at Hα, $\tau(\alpha)$, with their standard errors, have been determined simultaneously by the method presented by Gutiérrez-Moreno & Moreno (1996), using the reddening curve published by Seaton (1979). To obtain the absolute Hβ intensity, the observed flux was corrected by reddening and by self-absorption. This last correction was determined assuming that all the Hβ radiation comes from the nebula, without contribution from the core, and applying the numerical procedure suggested as a good first approximation by Ahern (1975).

The results are listed in Table 6, which gives, by column, (1) and (2) the name and year of the observation of the object; (3) log F(Hβ), corrected by the contamination produced by the Pickering series of He II; (4) the reddening constant at Hβ, Cβ, with its standard error; (5) the mean value of Cβ for each object, adopted in all the calculations that follow; (6) the optical depth at Hα, also with its standard error; when a negative value—always very close to 0—has been obtained for $\tau(\alpha)$, the value 0 has been adopted; (7) the reddening $E(B-V) = C\beta/1.47$; (8) the reddenings $E(B-V)$ given by other authors; (9) the value of $A_K = 0.37E(B-V)$ derived from (7); (10) the correction factor for self-absorption, C_s, with the standard errors derived from the observational errors; and (11) the logarithm of the absolute Hβ intensity, log I(Hβ), which includes the corrections for interstellar reddening and for self-absorption; standard errors are also listed.

As could be expected, and was already mentioned in a previous paper (Gutiérrez-Moreno et al. 1997), $\tau(\alpha)$ and C_s are well correlated. We have found a linear relation,

$$C_s = 1.023 + 0.078\tau(\alpha), \quad \sigma_{C_s} = \pm 0.016 ,$$

that allows a rapid estimate of C_s when $\tau(\alpha)$ is known.

4.2. Electron Temperatures and Densities

Because of the characteristics of the spectra of the objects we are studying, not many of the lines generally used for plasma diagnostics have been measured; the only line intensity ratio we have available is the nebular to auroral ratio of O III, $I(5007 + 4959)/I(4363)$. Since this ratio alone does not permit the determination of T_e and N_e, we have made an estimate of the electron temperatures and densities using the method given by Ferland & Shields (1978), which involves the lines of [O III] $\lambda\lambda$4959, 5007, 4363, [Ne III] λ3869, and He I λ5876. The use of their method allows the determination not only of the electron temperature and density of the nebula but also of the relative abundances N(O III)/N(Ne III) and N(O III)/N(He II). Nevertheless, we have observations of [Ne III] λ3869 in only a few cases, and we cannot combine the equations as proposed by Ferland & Shields (1978); thus we have used, in addition to the equation for [O III], only the equation involving the relation for $I(5007 + 4959)/I(5876)$. The use of this last relation implies the knowledge of the relative abundance $A = N$(O III)/N(He II), which is not known in advance. Thus, we have adopted as an initial value the abundance N(O)/N(He) found in the Sun (taken from de Freitas Pacheco et al. 1991): $A = 8.685 \times 10^{-3}$. This assumes that O III and He II are present in nearly coincident regions and that their relative abundances are equal to that of the corresponding ions, which is adequate since their ionization potentials are similar; then

$$\frac{N(\text{O III})}{N(\text{He II})} = \frac{N(\text{O})}{N(\text{He})} .$$

Besides, the method assumes Case B conditions for the region where the He I lines are formed.

The numerical coefficients included in relations (1) and (3) of Ferland & Shields (1978) have been modified according to the values of the atomic constants given by Mendoza (1983). We have found values of T_e and N_e with the adopted

TABLE 4

OBSERVED FLUXES (Hβ + Pi 8 = 100)

LINE (Å)	IDENTIFICATION	Hen 828		Hen 905	Hen 1103		Hen 1213			KX TrA	AE Ara	AS 255	
		1987	1991	1987	1987	1991	1987	1991	1995	1987	1991	1987	1991
3133	O III	...	...	...	...	3.73	...	...	...	...	...	...	...
3312	O III	...	...	...	...	1.91	...	...	...	...	...	...	...
3335	Ne II	...	...	...	...	6.53	...	...	...	...	...	...	...
3346	[Ne V]	...	...	...	...	...	...	...	...	...	7.49	...	...
3708	O III	...	...	...	...	...	...	...	...	...	8.90	...	...
3758	He II	...	...	...	...	...	...	...	...	...	8.36	...	...
3796	He II	...	...	...	...	2.61	...	...	...	...	...	...	...
3835	He II + H9	...	...	...	...	4.74	3.88	4.62	...	...	8.55	6.75	...
3869	[Ne III] + He I	6.69	...	...	...	...	3.62	2.07	...	6.90	27.8	...	...
3889	He I + H8	11.7	...	10.6	9.55	11.9	6.59	6.70	...	10.3	14.4	5.14	11.5
3968	[Ne III] + H7	13.4	...	13.4	10.4	7.87	8.56	8.25	...	10.5	26.3	10.2	8.87
4026	He II	...	...	...	...	...	...	...	...	1.74	...	...	...
4072	[S II]	...	...	...	...	...	...	...	...	1.20	...	...	...
4101	N III + Hδ	16.5	15.6	15.9	17.7	17.1	13.6	16.0	16.7	17.9	26.3	12.7	16.1
4200	He II	...	...	...	...	...	...	...	...	1.51	...	...	...
4340	Hγ	30.2	26.5	30.3	35.1	28.7	31.8	33.3	34.7	35.4	40.9	31.0	29.5
4363	[O III]	10.3	14.4	...	3.51	4.83	5.57	4.64	3.98	8.13	30.8	...	...
4388	He I	...	...	...	...	...	5.88	...	4.12	...	...	3.49	...
4471	He I	...	...	...	2.98	3.35	3.38	3.90	2.83	2.13	7.00	2.14	...
4542	He II	...	...	...	...	...	...	...	...	2.86	...	...	...
4640	N III	9.56	...	...	...	18.3	...	...	...	...	...	...	...
4647	C III	...	...	...	...	...	...	...	...	...	16.1	...	...
4686	He II	30.9	13.8	98.9	82.2	31.5	18.4	16.6	9.12	59.7	20.6	95.4	97.0
4712	[Ar IV] + He I	...	...	...	...	...	8.14	5.28	3.83	...	...	3.04	...
4861	Hβ	100	100	100	100	100	100	100	100	100	100	100	100
4922	He I	9.87	17.7	...	4.10	11.2	18.2	13.9	11.0	3.91	7.69	8.3	9.76
4945	[Fe VII]	...	...	...	...	...	...	...	...	5.32	...	...	...
4959	[O III]	8.36	...	...	...	...	...	...	...	6.81	29.1	...	...
5007	[O III]	25.0	...	...	...	22.6	3.66	4.03	2.92	23.4	86.5	...	...
5016	He I	6.99	20.7[a]	...	...	...	12.1	4.00	4.92	2.89	...	9.41	...
5048	He I	...	...	...	...	...	...	...	...	...	...	2.93	...
5159	[Fe VII]	2.66	...	2.13	...	...	5.15	...	4.42	5.00	...	...	...
5278	[Fe VII]	2.56	...	...	...	...	...	...	...	3.14	...	...	...
5309	[Ca V]	...	...	...	...	...	...	...	...	2.05	...	...	...
5412	He II	...	...	14.2	7.49	5.85	...	...	...	6.42	...	9.35	...
5615	[Ca VII]	...	...	...	...	...	...	...	...	5.98	...	...	...
5721	[Fe VII]	...	...	...	...	...	...	...	...	10.4	...	...	...
5807	He II	4.68	...	...	...	...	...	...	...	...	20.1	...	...
5876	He I	35.1	37.0	39.5	22.3	21.9	64.3	45.9	48.2	12.6	40.8	18.8	39.1
6087	[Ca V] + [Fe VII]	8.38	...	3.60	...	...	...	...	...	16.6	...	...	...
6311	He II + [S III]	...	...	...	...	...	...	...	...	2.05	...	...	...
6563	Hα	984	825	1224	767	548	831	729	587	943	562	806	1009
6678	He I	25.1	24.3	33.9	24.5	21.8	88.5	42.5	58.6	6.38	15.7	25.6	42.6
6825	O VI	...	...	119	54.2	...	...	...	...	49.4	...	41.9	119
7065	He I	39.0	...	46.0	...	17.5	77.8	30.2	...	13.0	26.4	15.4	57.4
7281	He I	...	...	...	...	5.57	...	...	...	...	...	...	...
10124	He II	...	...	...	...	...	...	...	...	...	...	...	40.8
−log F(Hβ)...		12.2	12.6	12.8	12.2	11.8	12.0	12.1	11.9	11.2	11.6	11.8	12.6

TABLE 4—*Continued*

Line (Å)	Identification	AS 270			AS 289		Y CrA	AS 304	AS 316		AS 327		CD −43°14304	
		1987	1991	1995	1987	1991	1990	1987	1987	1991	1987	1991	1987	1991
3133	O III	...	...	...	...	...	...	...	...	6.33	...	...	...	...
3203	He II	...	...	...	...	...	...	...	...	14.7	...	15.8	...	...
3341	O III + [Ne V]	...	...	...	...	...	89.8	...	...	...	...	...	...	...
3423	O III + [Ne V]	...	...	...	...	...	283	...	...	...	...	22.5	...	7.26
3429	O III	...	...	...	...	...	...	...	...	13.0	...	...	...	...
3499	He I	...	...	...	...	...	...	...	...	7.07	...	...	...	...
3586	[Fe VII] + He	...	...	...	...	...	19.7	...	...	...	...	...	...	...
3727	[O II]	...	...	...	...	...	11.3	...	...	...	...	...	...	...
3759	[Fe VII]	...	...	...	...	...	33.7	...	...	...	...	...	...	...
3835	He II + H9	...	...	...	...	...	...	12.6	3.90	4.01	2.66	...	...	...
3869	[Ne III] + He I	...	...	...	...	...	32.8	8.92	...	...	...	...	...	...
3889	He I + H8	...	...	...	3.62	...	15.1	22.7	7.40	8.00	5.40	9.60	5.96	11.3
3968	[Ne III] + H7	...	...	...	5.47	...	25.8	24.5	6.17	7.87	5.98	9.93	4.84	8.80
4026	He II	...	...	...	2.87:	...	...	5.62	...	...	3.53	...	5.69	4.65
4101	N III + Hδ	13.3	15.3	13.5	10.6	10.4	24.6	23.3	14.6	14.7	13.9	15.8	13.9	15.3
4200	He II	...	...	...	...	...	...	...	...	...	3.32	...	...	...
4340	Hγ	27.8	30.5	24.3	24.2	23.5	44.3	44.4	32.7	31.5	29.3	33.7	29.7	33.0
4363	[O III]	16.5	15.3	6.68	1.38	4.34	32.0	5.68	...	...	...	...	10.7	4.70
4388	He I	5.91	...	2.00	...	...	...	6.51	...	...	3.96	...	...	5.35
4415	[O II]	...	...	...	...	...	...	3.94	...	...	...	...	...	...
4471	He I	6.76	6.92	1.97	2.67	...	...	5.21	2.02	2.34	3.49	3.00	4.16	8.73
4542	He II	...	...	...	...	...	...	...	2.17	2.16	5.52	...	...	...
4647	C III	...	6.92	...	...	...	...	...	...	...	...	...	...	...
4686	He II	41.6	45.3	23.1	64.1	82.3	94.0	23.5	52.6	47.9	91.5	73.2	65.2	68.9
4712	[Ar IV] + He I	8.73	20.5	4.29	...	...	...	4.02	...	...	3.41	...	...	6.54
4716	[Ne IV]	...	...	...	...	...	9.12	...	...	...	...	...	...	...
4725	[Ne IV]	11.7	...	3.56	...	...	...	...	...	...	...	...	...	...
4740	[Ar IV]	...	...	...	...	...	11.5	...	...	...	...	...	...	...
4861	Hβ	100	100	100	100	100	100	100	100	100	100	100	100	100
4922	He I	18.6	64.6	5.89	8.38	...	...	15.0	6.18	10.1	6.14	11.1	3.79	12.0
5007	[O III]	30.4	26.2	9.84	2.18	...	103	9.16	1.17:	...	3.02:	...	...	...
5016	He I	9.63	...	5.11	8.69	...	...	14.4	4.63	4.64	8.68	2.62	8.49	10.1
5159	[Fe VII]	...	...	...	4.85:	...	...	...	...	...	4.78	...	...	...
5309	[Ca V]	...	...	...	...	...	10.5	...	...	...	...	...	...	...
5412	He II	...	...	...	12.9	28.7	27.2	...	7.16	6.29	10.9	10.1	...	8.47
5721	[Fe VII]	...	...	...	11.2	20.5	31.3	...	...	...	4.05	...	...	...
5876	He I	111	125	51.5	54.9	62.5	28.8	31.7	22.0	15.5	50.1	17.2	50.1	52.1
6087	[Ca V] + [Fe VII]	...	...	...	26.7	45.5	45.6	...	...	...	6.10	...	...	...
6528	He II	...	...	...	...	...	45.9	...	...	...	...	...	...	...
6563	Hα	1922	2325	1514	2152	2228	679	659	938	717	1133	903	897	631
6678	He I	115	160	79.2	91.6	114	12.8	31.8	18.3	14.4	58.8	23.0	58.0	28.7
6825	O VI	...	...	...	67.9	331	53.2	...	87.9	83.7	119	92.6	141	75.3
7065	He I	164	...	...	83.6	75.2	...	24.4	20.5	8.57	63.4	15.8:	37.6	38.6
9232	H I(Pa 9)	...	...	...	...	...	...	...	...	...	...	...	...	15.6
9403	?	...	...	...	...	...	...	...	...	...	...	...	...	32.4
10049	H I(Pa δ)	...	...	...	...	...	...	...	...	...	...	...	...	10.8
10124	He II	...	...	...	...	...	...	...	...	...	...	...	...	22.6
−log F(Hβ)...		13.0	13.0	12.5	12.0	12.7	12.9	11.5	11.8	11.8	12.3	12.2	12.1	11.6

[a] Badly blended with [O III] λ5007.

TABLE 5

SPECTRAL TYPE OF THE LATE COMPONENT AND DERIVED PARAMETERS

	SPECTRAL TYPE		DISTANCE (kpc)	
OBJECT (1)	This Paper (2)	Other (3)	This Paper (4)	Other (5)
Hen 828	M2.9 ± 0.4	M5.5[a]	1.6	2.2[a]
Hen 905	M4.3 ± 0.1	M2[a]	3.9	1.7[a]
Hen 1103.....	M1.3 ± 0.7		2.3	
Hen 1213.....	M0.0 ± 0.2		0.9	
KX TrA	M3.9 ± 0.6	M5.5,[a] M3[b]	1.2	3.8,[a] 3.0,[b] 4.4[c]
AE Ara	M4.4 ± 0.3	M3[b]	1.9	2.3,[b] 1.6[c]
AS 255	K5.2 ± 0.2		1.5	
AS 270	M4.3 ± 0.2		1.1	
AS 289	M3.3 ± 0.4		0.6	
Y CrA	M6.1 ± 0.1		2.9	3.9[c]
AS 304	M0.1 ± 0.8		1.3	2.5[d]
AS 316	M2.7 ± 0.2	M3[b]	1.7	4.5[b]
AS 327	M2.5 ± 0.4	M0[b]	1.9	3.0[b]
CD −43°14304.....	M0.3 ± 0.1	M0,[a] K5.5[e]	1.3	1.0[a]

[a] Harries & Howarth 1996.
[b] Mikolajewska et al. 1997.
[c] Pereira 1995.
[d] Munari & Buson 1993.
[e] Schmid & Nussbaumer 1993.

abundance ratio for all the objects analyzed, except for the 1987 observations of Hen 1213, for which we got solutions only for $A \leq 4.9 \times 10^{-3}$. A second approximation made using the ratio A determined with the values of T_e and N_e just obtained showed only small variations.

We have to consider that the values of T_e and N_e obtained by this method, although better than values arbitrarily adopted, must be considered only as rough estimates. In fact, in addition to the observational errors in the data, which in some cases may be large, and the possible error involved in the a priori adoption of a relative abundance N(O III)/N(He II), which may not be adequate, we have two sources of error that may be important: (*a*) in S-type symbiotic nebulae the He I lines may not be formed in the same region than the [O III] lines, and (*b*) Proga, Mikolajewska, & Kenyon (1994) have found that the assumption of Case B conditions for the region where He I lines are formed is not true for all S-type symbiotic systems.

For objects where [O III] λ5007 is too faint to be measured, we have adopted approximate temperatures $T_e =$ 15,000 K; in these cases, the values of N_e have been estimated from the diagnostic diagram by Gutiérrez-Moreno et al. (1995) as being of the order of $10^{9.5}$ cm^{-3}. If an object was observed in two or more different runs and observations of [O III] λ5007 were available in only one of them, the values of T_e and N_e obtained in that run were adopted for the other ones.

Our values of T_e and N_e, together with values published by other authors, are listed in columns (3)–(6) of Table 7.

4.3. Helium Abundance

Owing to the high density, large self-absorption corrections are expected. Collisional excitation corrections were performed following Peimbert & Torres-Peimbert (1987) before computing the He II abundances by the procedure followed by Gutiérrez-Moreno & Moreno (1996) and Gutiérrez-Moreno et al. (1997). The lines used were He I $\lambda\lambda$4471, 5876, and 7065; the emissivities for these lines were interpolated for the different values of T_e and N_e from the data computed by Almog & Netzer (1989) for $N_e = 10^4$, 10^6, 10^8, and 10^{10} and $T_e =$ 10,000 K. He I λ6678 was not used since few emissivities for this line are listed by Almog & Netzer (1989) for these high densities. Hγ was used as the reference line in order to diminish the effects of optical depth in the hydrogen lines, since we know that $\tau(\gamma) \approx 0.07\tau(\alpha)$. When He I λ7065 was not observed, we adopted for τ(3889) the values derived from previous observations of the same object, which may not be very adequate. For one object (Y CrA) we had only one observation, with no values for λ7065; thus, to have an estimate of He abundance we adopted the value of τ(3889) obtained for AE Ara, which has similar values of T_e and N_e. The resulting error in

TABLE 6

REDDENING AND RELATED PARAMETERS

Object (1)	Year (2)	log $F(H\beta)$ (3)	$C\beta$ (4)	Adopted (5)	$\tau(\alpha)$ (6)	$E(B-V)$ (7)	Other (8)	A_K (9)	C_s (10)	log $I(H\beta)$ (11)
Hen 828	1987	−12.2	1.49 ± 0.11	1.5	1.8 ± 1.0	1.0		0.4	1.2 ± 0.1	−10.7 ± 0.3
	1991	−12.6	1.55 ± 0.22		0				1	−11.1 ± 0.3
Hen 905	1987	−13.1	1.65 ± 0.07	1.6	3.1 ± 0.7	1.1		0.4	1.3 ± 0.1	−11.3 ± 0.2
Hen 1103	1987	−12.3	1.19 ± 0.01	1.2	1.5 ± 0.1	0.8		0.3	1.1 ± 0.1	−11.0 ± 0.1
	1991	−11.8	1.18 ± 0.22		0				1	−10.7 ± 0.3
Hen 1213	1987	−12.0	1.57 ± 0.08	1.3	0	0.9		0.3	1	−10.7 ± 0.2
	1991	−12.1	1.30 ± 0.00		0.3 ± 0.0				1.0 ± 0.0	−10.7 ± 0.1
	1995	−11.9	1.11 ± 0.01		0				1	−10.5 ± 0.1
KX TrA	1987	−11.2	1.28 ± 0.00	1.3	3.2 ± 0.0	0.9	0.03,[a] 0.82,[b] 0.8[c]	0.3	1.3 ± 0.1	−9.8 ± 0.1
AE Ara	1991	−11.6	0.52 ± 0.15	0.5	3.9 ± 1.8	0.3	0.00,[d] 0.5[c]	0.1	1.3 ± 0.2	−11.0 ± 0.4
AS 255	1987	−11.9	1.63 ± 0.10	1.6	0	1.1		0.4	1	−10.3 ± 0.2
	1991	−12.7	1.55 ± 0.12		1.6 ± 1.0				1.2 ± 0.1	−11.1 ± 0.3
AS 270	1987	−13.1	2.12 ± 0.01	2.1	4.4 ± 0.1	1.4		0.5	1.4 ± 0.1	−10.9 ± 0.1
	1991	−13.1	2.02 ± 0.00		9.2 ± 0.0				1.7 ± 0.1	−10.8 ± 0.1
	1995	−12.6	2.08 ± 0.16		1.8 ± 1.4				1.2 ± 0.2	−10.4 ± 0.4
AS 289	1987	−12.1	2.50 ± 0.01	2.5	2.1 ± 0.1	1.7		0.6	1.2 ± 0.1	−9.4 ± 0.1
	1991	−12.8	2.56 ± 0.01		2.0 ± 0.1				1.2 ± 0.1	−10.2 ± 0.1
Y CrA	1990	−12.4	0.63 ± 0.00	0.6	5.5 ± 0.0	0.4	0.23[d]	0.2	1.4 ± 0.1	−11.6 ± 0.1
AS 304	1987	−11.5	0.67 ± 0.04	0.7	4.6 ± 0.5	0.5	0.40[e]	0.2	1.4 ± 0.1	−10.7 ± 0.2
AS 316	1987	−11.8	1.54 ± 0.07	1.5	0.9 ± 0.5	1.0	0.7[c]	0.4	1.1 ± 0.1	−10.3 ± 0.2
	1991	−11.8	1.41 ± 0.00		0				1	−10.4 ± 0.1
AS 327	1987	−12.3	1.76 ± 0.01	1.6	1.1 ± 0.1	1.1	1.0[c]	0.4	1.1 ± 0.1	−10.7 ± 0.1
	1991	−12.2	1.42 ± 0.04		1.4 ± 0.3				1.1 ± 0.1	−10.6 ± 0.2
CD −43°14304	1987	−12.2	1.64 ± 0.01	1.5	0	1.0	<0.20[f]	0.4	1	−10.7 ± 0.1
	1991	−11.7	1.28 ± 0.02		0				1	−10.2 ± 0.1

[a] Feibelman 1991 (UV values).
[b] Pereira 1995.
[c] Mikolajewska et al. 1997.
[d] Nussbaumer et al. 1988 (UV values).
[e] Munari & Buson 1993.
[f] Schmid & Nussbaumer 1993 (UV values).

y^+ must not be large, since changes in the value of $\tau(3889)$ do not produce large variations in the emissivity of $\lambda 5876$.

The He III abundance was computed from He II $\lambda 4686$, using Brocklehurst (1971) emissivities extrapolated to our values of the density.

The results on He abundances are listed in columns (7)–(12) of Table 7, which give (7) the He^+ abundance, expressed as $y^+ = N(He^+)/N(H^+)$, obtained as the direct average of the lines used except when $I(7065)$ was not measured, in which case double weight was given to $y^+(5876)$; (8) the value of $y^{++} = N(He^{++})/N(H^+)$; (9) the total He abundance, $y = y^+ + y^{++} = N(He)/N(H)$. Columns (10), (11), and (12) list the same values as listed by Pereira (1995). The errors in y^+ and y^{++} are given in units of the last decimal; since we have used only one line for the determination of y^{++}, the error quoted in this case is an estimate based on the mean error of the measures of this line. Since the values of T_e and N_e are only estimates, the real errors may be quite larger than those quoted here.

Comparison of our values with Pereira's (1995) for the objects in common shows large differences in y^+, y^{++}, and y; they may be due to the differences in reddening and the consequent differences in T_e and N_e, but they are large enough to suspect that some variability may be present. In fact, treating Pereira's (1995) data with our procedures gives slightly larger He abundances, but the differences with our values are still too large to be explained only by the observational errors.

5. THE HOT SOURCES

5.1. Magnitudes

B and V magnitudes were obtained for all objects observed by convolving the intensities measured in each spectrum—without considering the emission lines due to the nebula—with the sensitivity functions of Johnson's B and V filters. The results are listed in Table 8, which gives the magnitudes thus determined and the corresponding $B-V$ colors; the errors listed for B and V are the mean errors of the average of the magnitudes obtained for each object and epoch. The table includes also the values listed

TABLE 7

NEBULAR PARAMETERS

		T_e		log N_e		THIS PAPER			OTHER		
OBJECT (1)	YEAR (2)	This Paper (3)	Other (4)	This Paper (5)	Other (6)	y^+ (7)	y^{++} (8)	y (9)	y^+ (10)	y^{++} (11)	y (12)
Hen 828	1987	10700	...	7.9	...	0.079 ± 0.001	0.037 ± 0.001	0.116	...	...	...
	1991	10700	...	7.9	...	0.080 ± 0.011	0.019 ± 0.003	0.099	...	...	...
Hen 905	1987	15000	...	9.5	...	0.061 ± 0.002	0.142 ± 0.001	0.203	...	...	...
Hen 1103	1987	9300	...	7.6	...	0.063 ± 0.001	0.088 ± 0.004	0.151	...	...	...
	1991	9300	...	7.6	...	0.085 ± 0.004	0.040 ± 0.001	0.125	...	...	...
Hen 1213	1987	15700	...	9.1	...	0.099 ± 0.006	0.024 ± 0.002	0.123	...	...	...
	1991	13800	...	9.1	...	0.091 ± 0.003	0.014 ± 0.001	0.105	...	...	...
	1995	14900	...	9.3	...	0.082 ± 0.010	0.011 ± 0.003	0.093	...	...	...
KX TrA	1987	10500	16000[a]	7.7	6.4[a]	0.037 ± 0.005	0.062 ± 0.003	0.099	0.64[a]	0.036[a]	0.100[a]
AE Ara	1991	10000	10500[a]	7.5	7.0[a]	0.161 ± 0.005	0.021 ± 0.001	0.182	0.80[a]	0.012[a]	0.092[a]
AS 255	1987	15000	...	9.5	...	0.036 ± 0.004	0.136 ± 0.008	0.172	...	...	...
	1991	15000	...	9.5	...	0.058 ± 0.000	0.145 ± 0.001	0.203	...	...	...
AS 270	1987	11900	...	8.3	...	0.170 ± 0.004	0.051 ± 0.005	0.221	...	...	...
	1991	12100	...	8.4	...	0.163 ± 0.011	0.050 ± 0.001	0.213	...	...	...
	1995	12800	...	8.5	...	0.068 ± 0.009	0.033 ± 0.003	0.101	...	...	...
AS 289	1987	13000	...	9.1	...	0.058 ± 0.002	0.091 ± 0.003	0.149	...	...	...
	1991	13000	...	9.1	...	0.073 ± 0.000	0.122 ± 0.011	0.195	...	...	...
Y CrA	1990	10200	13000[a]	7.4	6.5[a]	0.103 ± 0.005	0.088 ± 0.004	0.191	0.048[a]	0.037[a]	0.085[a]
AS 304	1987	10400	...	8.4	...	0.098 ± 0.002	0.024 ± 0.003	0.122	...	...	...
AS 316	1987	13400	...	9.2	...	0.038 ± 0.000	0.068 ± 0.003	0.106	...	...	...
	1991	13400	...	9.2	...	0.031 ± 0.007	0.065 ± 0.002	0.096	...	...	...
AS 327	1987	17100	...	9.3	...	0.078 ± 0.004	0.129 ± 0.001	0.207	...	...	...
	1991	17100	...	9.3	...	0.037 ± 0.009	0.088 ± 0.002	0.125	...	...	...
CD −43°14304	1987	15000	...	9.5	9[b]	0.083 ± 0.004	0.094 ± 0.004	0.177	...	...	...
	1991	15000	...	9.5	...	0.108 ± 0.001	0.098 ± 0.002	0.206	...	...	...

[a] Pereira 1995.
[b] Schmid & Nussbaumer 1993.

by Munari et al. (1992) for some of our objects. As could be expected by not including the emission lines, our magnitudes are in general fainter than theirs.

5.2. Temperature, Luminosities, and Radii

We have estimated the radiation temperature of the hot sources by the method proposed by Iijima (1981); the values obtained may be considered upper limits. The results are listed in Table 9, together with some values presented by other authors. We have estimated errors of 7% in the mean for our temperatures. Mikolajewska, Acker, & Stenholm (1997) obtain the temperatures by the procedure suggested by Mürset & Nussbaumer (1994), who use a simple formula that relates the temperature of the hot component with the highest ionization potential observed in the nebular spectrum.

The luminosity was estimated by the method of Zijlstra & Pottasch (1989), using the line He II λ4686 instead of Hβ:

$$\frac{4\pi d^2 I(\text{He II})}{L^*} = h\nu(\text{He II})\,\frac{\alpha(\text{He II})}{\alpha_B} \times \frac{15 G_4(T^*)}{\pi^4 k T^*} ,$$

where I(He II) is the He II λ4686 flux corrected for reddening; α(He II) is the total recombination coefficient for He II λ4686, whereas α_B is the effective recombination coefficient for the same line; and $G_4(T^*)$ is the Zanstra temperature integral for He II λ4686. The values of $G_4(T^*)$, α(He II), and α_B have been tabulated (see, for example, Pottasch 1984). Knowing the luminosity, the radius may be easily estimated from the relation

$$L^*/L_\odot = (R^*/R_\odot)^2 (T^*/T_\odot)^4 .$$

The results obtained are listed in Table 9, which gives, for each object and each epoch of observation, in addition to the temperatures, the corresponding radii and luminosities and results obtained by other authors.

We have estimated errors of the order of 40% in the mean for the luminosities and radii, but the real errors may be much larger than these, since they not only depend on the errors of the temperatures quoted before, but also depend very strongly on the errors of the distances.

Since we have used the upper limit for T^*, the radius and luminosity listed are both lower limits.

TABLE 8

B AND *V* MAGNITUDES

		This Paper			Other		
Object	Year	*B*	*V*	*B*−*V*	*B*	*V*	*B*−*V*
Hen 828	1987	15.52 ± 0.02	14.90 ± 0.11	0.62	15.19	14.29	0.90
	1991	14.28 ± 0.10	14.08 ± 0.06	0.20	…	…	…
Hen 905	1987	16.70 ± 0.02	15.43 ± 0.04	1.27	15.80	14.16	1.64
Hen 1103	1987	15.56 ± 0.12	14.52 ± 0.03	1.04	14.00	13.20	0.80
	1991	13.05 ± 0.01	12.82 ± 0.01	0.23	…	…	…
Hen 1213	1987	14.15 ± 0.12	12.75 ± 0.06	1.40	…	…	…
	1991	14.29 ± 0.08	12.81 ± 0.08	1.48	…	…	…
	1995	14.11 ± 0.10	12.79 ± 0.04	1.32	…	…	…
KX TrA	1987	14.78 ± 0.11	14.35 ± 0.19	0.43	…	…	…
AE Ara	1987	13.60 ± 0.12	13.48 ± 0.06	0.12	12.66	12.14	0.52
AS 255	1987	14.47 ± 0.04	13.31 ± 0.05	1.16	14.75	13.01	1.74
	1991	15.11 ± 0.06	13.67 ± 0.01	1.44	…	…	…
AS 270	1987	16.62 ± 0.11	14.75 ± 0.11	1.87	15.70	13.71	1.99
	1991	16.29 ± 0.08	14.67 ± 0.08	1.62	…	…	…
	1995	15.96 ± 0.08	14.56 ± 0.04	1.40	…	…	…
AS 289	1987	15.72 ± 0.19	13.81 ± 0.04	1.91	15.72	13.62	2.10
	1991	16.34 ± 0.10	14.35 ± 0.04	1.99	…	…	…
Y CrA	1990	15.50 ± 0.12	14.71 ± 0.06	0.79	15.56	14.35	1.21
AS 304	1987	12.23 ± 0.08	12.06 ± 0.08	0.17	11.69	11.19	0.50
AS 316	1987	15.12 ± 0.05	13.89 ± 0.04	1.23	…	…	…
	1991	15.48 ± 0.12	14.41 ± 0.08	1.07	…	…	…
AS 327	1987	15.23 ± 0.10	13.99 ± 0.02	1.24	14.43	12.89	1.54
	1991	15.30 ± 0.12	13.88 ± 0.04	1.42	…	…	…
CD −43°14304	1987	13.70 ± 0.01	12.53 ± 0.04	1.17	13.12	11.55	1.57
	1991	13.19 ± 0.08	12.14 ± 0.02	1.05	…	…	…

Figure 15 presents the location of the objects observed in the H-R diagram. For each object with several observations we have used the average of the temperatures and luminosities obtained, except in the cases of Hen 828 and Hen 1103, for which the variations seem to be real. The objects indicated by a dot have He abundances greater than 0.17.

6. DISCUSSION OF SOME INDIVIDUAL OBJECTS

6.1. Hen 828

There is a notorious increase of the level of the continuum between 1987 and 1991, and, as can be seen in Figure 1 and Table 4, many of the emission lines visible in 1987 have become undetectable in 1991, as if being veiled by the high level of the continuum; the lines that remain visible are mainly recombination lines; the only exceptions are the [O III] lines λ4363 and λ5007, which are visible but have not been measured since they are completely blended with He I λ5016. The dereddened 1991 spectrum (Fig. 16) shows a continuum with a maximum (≈3200–3400 Å), which suggests a temperature of the order of 7500–8500 K, corresponding an A5–F0 star. These changes suggest that the object was having an outburst in 1991. Table 8 shows that Hen 828 was brighter in both *B* and *V* during this outburst than in 1987; nevertheless, the resulting total luminosity was smaller for the 1991 observations, because of the faintness of He II λ4686.

6.2. Hen 905

In the second-order spectrum of Hen 905, an emission located at a distance of about 2′ to the west of the central object was detected in both Hα and O VI λ6825. The region between the object and this emission is full of faint emissions, which extend also to the east of the object, as shown in Figure 17, which corresponds to O VI λ6825. The minimum *X*-value of the plot is fixed at 0 and does not allow us to see the point symmetrical to the west emission; this fact suggests that there could be another emission at the east of the object, which would imply the existence of a ring surrounding the central object, and emitting mainly in Hα and O VI. The emission in Hα (≈20) is more intense than in O VI λ6825 (≈15) but is less conspicuous in the corresponding graph, since the intensity relative to the central line (≈$\frac{1}{6}$) is much smaller than in the case of λ6825.

The emission in λ6825 in the one-dimensional spectrum is fairly intense and wide, suggesting several components.

TABLE 9

TEMPERATURE, RADIUS, AND LUMINOSITY OF THE HOT COMPONENTS

		T^*		log $L/L_\odot$		$R/R_\odot$	
OBJECT	YEAR	This Paper	Other	This Paper	Other	This Paper	Other
Hen 828	1987	130,000	...	2.38	...	0.031	...
	1991	108,000	...	1.88	...	0.025	...
Hen 905	1987	182,000	...	2.77	...	0.025	...
Hen 1103	1987	183,000	...	2.54	...	0.019	...
	1991	131,000	...	2.80	...	0.049	...
Hen 1213	1987	112,000	...	1.84	...	0.022	...
	1991	109,000	...	1.80	...	0.022	...
	1995	96,000	...	1.91	...	0.033	...
KX TrA	1987	165,000	114[a]	3.04	3.9[a]	0.041	...
			140–150[b]	...	2.8[b]	...	...
AE Ara	1991	111,000	54–80[a]	2.10	3.0[a]	0.031	...
			70–105[b]	...	0.9[b]	...	...
AS 255	1987	198,000	...	3.04	...	0.028	...
	1991	205,000	...	3.15	...	0.030	...
AS 270	1987	141,000	...	1.76	...	0.013	...
	1991	145,000	...	1.79	...	0.013	...
	1995	124,000	...	2.15	...	0.026	...
AS 289	1987	174,000	...	0.90	...	0.003	...
	1991	182,000	...	1.23	...	0.004	...
Y CrA	1990	190,000	130–140[b]	2.15	2.4[b]	0.011	...
AS 304	1987	117,000	>65[c]	2.06	>3.9[c]	0.026	<0.68[c]
AS 316	1987	159,000	114[a]	2.89	3.3[a]	0.037	...
	1991	152,000	...	2.87	...	0.039	...
AS 327	1987	192,000	114[a]	2.77	3.4[a]	0.022	...
	1991	177,000	...	2.82	...	0.028	...
CD $-43°14304$	1987	167,000	...	2.38	...	0.019	...
	1991	162,000	...	2.93	...	0.037	...

[a] Mikolajewska et al. 1997.
[b] Pereira 1995.
[c] Munari & Buson 1993.

6.3. Hen 1103

The behavior of the continuum in this object is similar to that of Hen 828, since it is higher in 1991 than in 1987. The dereddened spectra also behave like those of Hen 828, in the sense that in 1991 the continuum has an A–F spectrum (Fig. 18). It is difficult to estimate its temperature, since the Balmer continuum is in emission, which does not allow a good judgment of the maximum intensity.

We consider that, as Hen 828, Hen 1103 was also having an outburst in 1991. There is, however, a difference between both objects, since the emission lines of Hen 1103 show no major changes between both dates of observation.

6.4. Hen 1213

This object was observed in the UV in 1995 (Gutiérrez-Moreno et al. 1997); the observations were severely affected by an extraordinarily high radiation level, but it was possible to state that lines of C IV, He II, and C III] were present.

6.5. KX TrA

According to Feibelman (1988) the low-dispersion *International Ultraviolet Explorer* (*IUE*) spectra of this object resemble strongly to V1016 Cyg and HM Sge; he states that the characteristics of the UV spectra suggest a high-excitation object containing a very hot star. The high excitation is also noticeable in the visual spectrum, rich in emission lines. There is a large difference between the reddening obtained by the Balmer decrement method and that obtained in UV, from the absence of the λ2200 feature (Feibelman 1988); this low UV reddening is in agreement with the comment by Webster (1973) that the region is free of nebulosity and dust lanes and that any reddening is more likely due to circumstellar dust rather than interstellar dust. Determination of the reddening by using the He II lines in

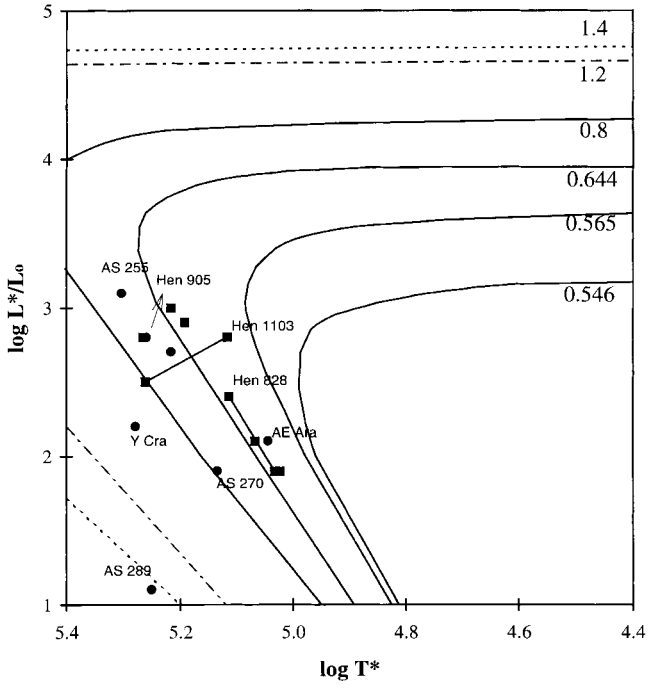

FIG. 15.—H-R diagram of the objects observed. The curves are evolutionary tracks for stars of different masses (indicated at the right in units of $M_{\odot}$), as presented by Schönberner (1981; 0.546–0.644), Paczynski (1971; 0.8 and 1.2), and Shaw (1988; 1.4). Dots represent objects with $y \geq 0.17$—which have been identified—whereas squares correspond to objects with $y < 0.17$.

the visual (λ4686) and in UV (λ1640) gives $C\beta = 0.48$, which is close to the mean between the visual and UV values of $C\beta$.

6.6. AS 255

The dereddened spectra show that the continua corresponding to 1987 and 1991 have practically the same shape,

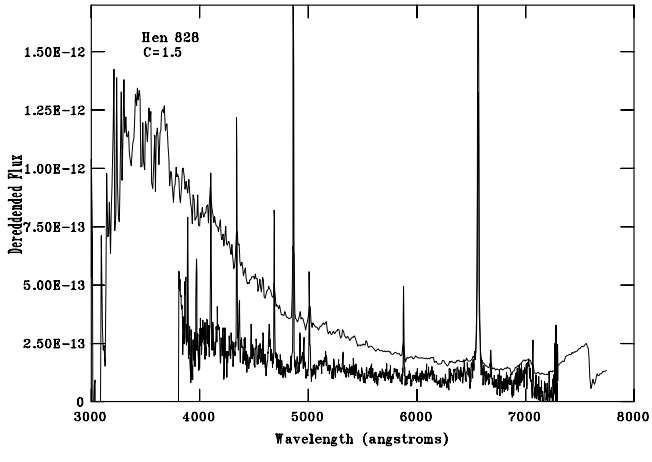

FIG. 16.—Dereddened spectra of Hen 828. The two spectra have the same zero point (separation step = 0).

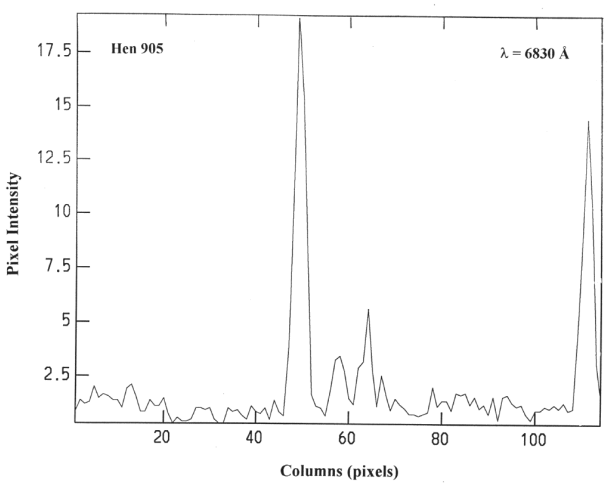

FIG. 17.—Tracing of the two-dimensional spectrum of Hen 905 through the lines O VI λ6825. It shows an emission within about 2″ of the main object, with faint emissions in between.

but the 1987 spectrum is slightly brighter than that of 1991. There is also a large difference in the intensity of the Balmer lines, which may be appreciated for Hβ in Tables 4 and 6.

6.7. AS 270

The dereddened spectra corresponding to 1987 and 1991 have practically identical continua, but that corresponding to 1995 shows an increase of the intensity shortward of 5000 Å; at 4000 Å the continuum intensity is about 3 times that of 1987. This fact suggests that the 1995 observations could also correspond to an outburst. Besides, the H lines are about twice as intense in the 1995 spectrum than in 1987 and 1991, whereas the observed fluxes of the other lines remain quite similar to those of the preceding epochs. This fact produces the decrease of the relative intensities of the lines of He I and He II, shown in Table 4, and the conse-

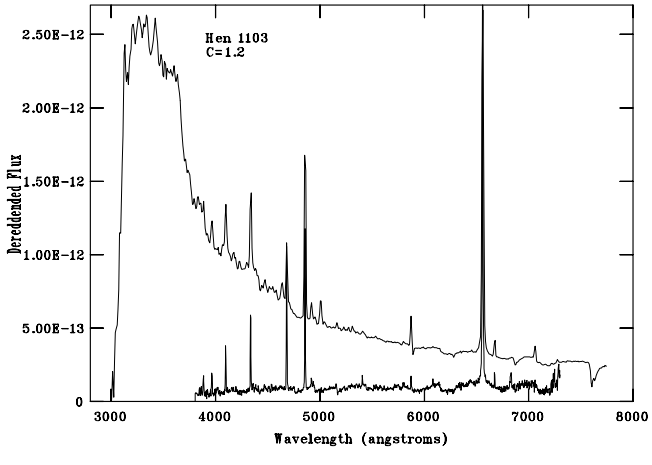

FIG. 18.—Same as Fig. 16, for Hen 1103

quent strong changes in the relative He abundance, shown in Table 7.

6.8. AS 289

The large intensity of Balmer lines, and mainly of Hβ, in 1987, produces the difference in the relative He abundance, presented in Table 7.

According to Figure 15, the progenitor star of the hot component of this objects is the most massive of the sample.

6.9. AS 304

Munari & Buson (1993) have analyzed *IUE*, optical, and infrared observations of this object. They find that the *IUE* spectra indicate that the hot component is losing mass at a high rate via a fast wind, being in this sense similar to the mass-losing nuclei of planetary nebulae (PNe).

They present a graph of the dereddened spectral energy distribution, which combines the *IUE* continuum fluxes with *JHKL* data, obtained almost simultaneously with the *IUE* observations, and with the $UBV(RI)_c$ photometry obtained by Munari et al. (1992). The distribution obtained matches perfectly that of a bulge M4 giant longward of 7000 Å, but departs from it at the *R* band and shortward, due to the presence of the strong nebular continuum, which goes far into the red. The temperature, luminosity, and radius estimated by Munari & Buson (1993) correspond to the He II Zanstra temperature.

6.10. AS 327

In this case, the variation in the He content reflects a real variation of the He lines, mainly λ5876, and not a variation of the H lines intensity.

6.11. CD −43°14304

The object was classified by Schmid & Nussbaumer (1993) as a metal-poor yellow symbiotic. Schmid et al. (1998) have obtained a series of high-resolution optical spectra of this object, deriving the radial velocity curve of the cool component and an orbital period of about 1448 days. The hot component was also detected with *ROSAT* as a very soft X-ray source (Mürset, Wolff, & Jordan 1997).

The dereddened spectra corresponding to 1991 June and July are slightly brighter than that corresponding to 1987; besides, both of them, show an increase of the intensity shortward of 5000 Å, being the intensity at 4000 Å in 1991 about 3 times that of 1987. This fact suggests that the objects was having a mild outburst in 1991.

7. GENERAL DISCUSSION

We presented here observations of 14 S-type symbiotic stars, obtaining some of their physical parameters. These parameters are full of uncertainties, which start with the observational errors of the measures—due mainly to the difficulty in the tracing of the continuum—and the many uncertainties already mentioned in the determination of the distances. For example, using Tsuji (1978) scale of bolometric magnitudes for M-type giants and the relevant data from Dyck, Lockwood, & Capps (1974) instead of Frogel & Whitford's (1987) scale, we get distances that are about twice as large as those listed in this paper; these errors have strong influence in the determination of the luminosities and, consequently, in the obtention of the radii.

Another source of errors is the adopted value of the reddening, with strong effects in many of the results obtained here. We must stress the large differences observed in some cases between optical and UV values, with the optical values being larger than those obtained with UV measures. This effect has been discussed elsewhere (Gutiérrez-Moreno et al. 1997), an in this paper it affects mainly KX TrA and AE Ara and may be some other objects for which no UV observations are available. It may be that, as Feibelman (1988) suggests, the difference is due to circumstellar reddening present in these objects; this would imply that this circumstellar reddening is not detected in the UV.

A further comment concerning the reddening determination is that reddenings obtained from the ratio $F(1640)/F(4686)$ of He II have to be taken with care, since when the UV reddening obtained independently of the visual observations—as is the case when the λ2200 feature is used—and the reddening in the optical region are different—as found here for KX TrA—the result obtained with the He II method is a combination of both values of Cβ, and does not represent the real reddening.

Partial corrections for collisional effects were used for the determination of the He II abundances ($\gamma \leq 0.3$, according to Peimbert & Torres-Peimbert notation). The value of γ was chosen so as to get the best agreement between the abundances obtained for the different lines used. Nevertheless, the corrections are very small when Almog & Netzer (1989) emissivities are used; this indicates that their method takes very well into account the collisional corrections.

The H-R diagram presented in Figure 15 shows some evolutionary tracks for the hot components of central stars of PNe. Our objects are located in positions similar to those

of rather evolved PNe nuclei. They show a large scatter both in T^* and L^*, with 96,000 $K < T^* < 205{,}000$ K for Hen 1213 (1995 observation) and AS 255, respectively; and $1.0 < \log L/L_\odot < 3.2$, for AS 289 and AS 255, respectively. It is noticeable that the all objects with high He contents—with the exception of AE Ara—are located to the left of the evolutionary track corresponding to $M^* = 0.644\ M_\odot$, suggesting rather massive progenitors.

On the other hand, a look at the radii of the hot components given in Table 9, even considering possible errors of the order of a factor of 2 (due to the uncertainties of the distances), shows that they seem to be all white dwarfs.

We are indebted to M. Smith of CTIO for the use of the Observatory facilities, and to the Visitors Support Group for their assistance during the observations. We acknowledge M. Hamuy for his help with the IRAF reductions at the Computing Center of CTIO at La Serena, and J. García for his help with the 1991 observations. We are also indebted to H. Pulgar for his assistance at the CPDI of the Departamento de Astronomía, and G. Cortés for her help in the handling of the data and preparation of the electronic version of the manuscript. We specially thank the anonymous referee for his valuable suggestions.

REFERENCES

Ahern, F. J. 1975, ApJ, 197, 639
Allen, D. A. 1982a, in IAU Colloq. 70, The Nature of Symbiotic Stars, ed. M. Friedjung & R. Viotti (Dordrecht: Reidel), 27
———. 1982b, in IAU Colloq. 70, The Nature of Symbiotic Stars, ed. M. Friedjung & R. Viotti (Dordrecht: Reidel), 115
Almog, Y., & Netzer, H. 1989, MNRAS, 238, 57
Brocklehurst, M. 1971, MNRAS, 153, 471
de Freitas Pacheco, J. A., Maciel, W. J., Costa, R. D. D., & Barbuy, B. 1991, A&A, 250, 159
Dyck, H. M., Lockwood, G. W., & Capps, R. W. 1974, ApJ, 189, 89
Feibelman, W. A. 1988, ApJ, 319, 407
———. 1991, ApJ, 375, 335
Ferland, G. J., & Shields, G. A. 1978, ApJ, 226, 172
Frogel, J. A., & Whitford, A. E. 1987, ApJ, 320, 199
Gutiérrez-Moreno, A., & Moreno, H. 1996, PASP, 108, 972
Gutiérrez-Moreno, A., Moreno, H., & Cortés, G. 1995, PASP, 107, 462
Gutiérrez-Moreno, A., Moreno, H., Costa, E., & Feibelman, W. A. 1997, ApJ, 485, 359
Hamuy, M., Walker, A. R., Suntzeff, N. B., Gigoux, P., Heathcote, S. R., & Phillips, M. M. 1992, PASP, 104, 533
Harries, T. J., & Howarth I. D. 1996, A&AS, 119, 61
Iijima, T. 1981, in Photometric and Spectroscopic Binary Systems, ed. E. B. Carling & Z. Kopal (Dordrecht: Reidel), 517
Kenyon, S. J. 1986, The Symbiotic Stars (Cambridge: Cambridge Univ. Press)
Kenyon, S. J., & Fernández-Castro, T. 1987, AJ, 938
Mendoza, C. 1983, in IAU Symp. 103, Planetary Nebulae, ed. D. R. Flower (Dordrecht: Reidel), 245
Mikolajewska, J., Acker, A., & Stenholm, B. 1997, A&A, 327, 191
Munari, U., & Buson, L. M. 1993, MNRAS, 263, 267
Munari, U., Yudin, B. F., Taranova, O. G., Massone, G., Marang, F., Roberts, G., Winkler, H., & Whitelock, P. A. 1992, A&AS, 93, 383
Mürset, U., & Nussbaumer, H. 1994, A&A, 282, 586
Mürset, U., Wolf, B., & Jordan, S. 1997, A&A, 306, 477
Nussbaumer, H., Schild, H., Schmid, H. M., & Vogel, M. 1988, A&A, 198, 179
Paczynski, B. 1971, Acta Astron., 21, 417
Peimbert, M., & Torres-Peimbert, S. 1987, Rev. Mexicana Astron. Astrofis., 14, 540
Pereira, C. B. 1995, A&AS, 111, 471
Pottasch, S. R. 1984, Planetary Nebulae (Dordrecht: Reidel)
Proga, D., Mikolajewska, J., & Kenyon, S. J. 1994, MNRAS, 268, 213
Schmid, H. M., & Nussbaumer, H. 1993, A&A, 268, 159
Schmid, H. M., Dumm, T., Mürset, U., Nussbaumer, H., Schild, H., & Schmutz, W. 1998, A&A, 329, 986
Schönberner, D. 1981, A&A, 103, 119
Seaton, M. J. 1979, MNRAS, 187, 73P
Shaw, R. A. 1988, IAU Symp. 131, Planetary Nebulae, ed. S. Torres-Peimbert (Dordrecht: Reidel), 473
Stone, R. P. S., & Baldwin, J. A. 1983, MNRAS, 204, 347
Taylor, B. J. 1984, ApJS, 54, 259
Terndrup, D. M., Frogel, J. A., & Whitford, A. E. 1990, ApJ, 357, 453
Tsuji, T. 1978, A&A, 62, 29
Turnshek, D. E., Turnshek, D. A., Craine, E. R., & Boeshaar, P. C. 1985, An Atlas of Digital Spectra of Cool Stars (Tucson: Western Research Co.)
Webster, L. 1973, MNRAS, 164, 381
Whitelock, P. A., & Munari, U. 1992, A&A, 255, 171
Zijlstra, A. A., & Pottasch, S. R. 1989, A&A, 216, 245